Catalytic Degradation of Organic Dyes using Synthesized Silver Nanoparticles: A Green Approach

Bhakya S[1], Muthukrishnan S[2]*, Sukumaran M[1], Muthukumar M[2], Senthil Kumar T[3] and Rao MV[2]

[1]Research Department of zoology, Rajah Serfoji Govt. College (Autonomous), Thanjavur- 613 005, Tamil Nadu, India
[2]*Department of Plant Science, Bharathidasan University, Tiruchirappalli-620 024, Tamil Nadu, India
[3]Department of Industry University Collaboration, Bharathidasan University, Tiruchirappalli 620 024, Tamil Nadu, India

Abstract

The scientific community is search in for new methods for the synthesis of metallic nanoparticles. Green synthesis has now become a vast developing area of new research groups. Here we report a green method to the synthesis of silver nanoparticles (AgNPs) using the different parts of Vishanika or Indian screw tree, an ayurvedic medicinal tree. This is nontoxic, eco-friendly and low cost method. The reduction and stabilization capability of the plant extracts of different parts are described. The size and structure of the silver can be characterized by varying the plant parts of the vishanika. The biosynthesized nanoparticles are characterized by using UV–VIS spectroscopy, TEM, XRD, DLS and FTIR. The size and extract dependent catalytic activity of the biosynthesized nanoparticles is established in the degradation of organic dyes.

Keywords: Green synthesis; *Helicteres isora;* Organic dyes; Silver nanoparticles; Degradation; Size dependent

Introduction

Organic dyes is one of the major groups of pollutants widely used in textile, plastic, medicine and many other industries, while the hazardous effects of organic dyes in waste water have been a major concern and now a major threat in the environment due to the substantial pollution problems caused by them. These industries exhausted large quantity of high content color effluents, which are generally more toxic and resistant to destruction by conventional methods. A necessary criterion in the use of these dyes is that they must be highly accumulated in water and stable in light during washing. The accumulation of these dyes in the water bodies causes eutrophication, reduces the reoxygenation capacity and makes severe damage to the aquatic organisms by hindering the infiltration of sunlight [1]. They must also be resistant to microbial attack. Therefore, they are not readily degradable and are typically not removed from water by wastewater treatment systems and conventional methods like adsorption, ultrafiltration, chemical and electrochemical methods [2]. The superiority of photocatalytic degradation by nanoparticles in wastewater treatment is due to its advantages over the conventional methods, such as quick oxidation, no formation of polycyclic products and oxidation of pollutants. It is an effective and rapid technique in the removal of pollutants from wastewater [3]. In the recent years, numerous metal oxides including TiO_2 [4], ZnO [5], and other oxides have attracted growing attentions for photodegradation of organic dyes; TiO_2 is of particular interests due to its low cost and high stability. Nonetheless, TiO_2 has a relatively large energy band-gap and only absorbs UV region, while the UV lights only contribute to less than 10% of total solar radiations; the visible lights, on the other hand, contribute to 50% of the solar radiations. It's a crucial drawback in photo-catalysts of TiO_2 based application [6]. So, in the recent years have been many research efforts devoted to improve the photocatalytic activity by incorporating of metal particles (silver, gold and iron) [7-9]**,** to broaden the absorption of solar radiations by doping with nitrogen and to reactivate the TiO_2-based photo-catalysts by treating with heat [10,11]. An alternative type of catalysts for photo-degradation of organic dyes is nanoparticles of some transition metals such as silver. The size, shape, large surface area to volume ratio and mass dependent reactivity has made metal nanoparticles high photo-catalytic activities [12]. Nowadays biosynthesis nanocatalysts are widely used for the effective removal of dye contaminants.

Among the many possible natural products, biologically active plant products represent excellent platforms for this purpose [6-8,13]. The compounds present in plants that have different potential biological activities; phytochemicals are important natural resource for the synthesis of metal nanoparticles. They play important roles in both stabilization and reduction of nanoparticles. The focus of the present work is to apply the accurate principles of green chemistry for the synthesis of silver nanoparticles by using stem bark, root and leaf of *Helicteres isora* extracts as stand-alone reducing and capping agent. *H. isora* plant extracts possess anticancer properties [14]. Usually, the bark and root juice were used against diabetes and emphysema. In traditional medicine, the bark and root juice is claimed to be useful in snake bite, diabetes, blood disorder, cough, colic, diarrhoea, astringent, etc., [15], expectorant and astringent [16], hypolipidemic [17], antihyperglycemic activity and glibenclamide [18]. In the present study, we have investigated the extracts and size dependent catalytic degradation of organic dyes–methyl violet, safranin, eosin methylene blue and methyl orange by in the presence of silver colloids.

Materials and Methods

Silver nitrate (99.99%), methyl violet, safranin, eosin methylene blue and methyl orange, were purchased from sigma Aldrich. All glassware's were cleaned with sterile distilled water and rinsed with deionized water.

Preparation of extract

Different parts of (stem bark, root and leaf) *H. isora* were collected from Western Ghats of Tamil Nadu, washed with sterile distilled water and dried, then make it powder. 1 g of each explants powder was mixed with 100 mL of water and kept on orbital shaker at 120 rpm for 12 h.

*Corresponding author: Muthukrishnan S, Department of Plant Science, Bharathidasan University, Tiruchirappalli-620 024, Tamil Nadu, India, Tel: +91 0431-240-7072; E-mail: muthukrishnan1985@gmail.com

After that, the extracts were filtered with filter paper and stored at 4°C in refrigerator until further use.

Synthesis of silver nanoparticles

Silver nanoparticles (stem bark (S), root (R) and leaf (L)) have been synthesized by Bhakya et al. [19] method with slight modification. The formation of AgNPs is indicated by the appearance of dark brown color within 5 min.

Characterization

UV–visible spectra analysis was performed for all samples and the absorption maxima were analyzed at a wavelength of 200–700 nm using UV–visible spectrophotometer (UV-160 v, Shimadzu, Japan). The biosynthesized AgNPs were examined for the presence of biomolecules using FTIR spectrum (Thermo Scientific Nicolet 380 FT-IR Spectrometer). The crystalline nature of particles was evaluated by using X-ray diffraction method (XRD). The studies on size and shape of silver nanoparticles were performed by transmission electron microscopy (JEOL JEM2100 TEM). To determine the size distribution of nanoparticles of colloidal solution was analyzed by the DLS particle size analyzer [ZETA Seizers Nanoseries (Malvern Instruments Nano ZS with Zetasizer Ver. 6.20)].

Catalytic activity of silver nanoparticles

The photocatalytic (in presence of sun light) activities of biogenic silver nanoparticles were studied for degradation methyl violet (MV), safranin (S), eosin methylene blue (EMB) and methyl orange (MO) at 50 mg/mL. The degradation of methyl violet (MV), safranin (S), eosin methylene blue (EMB) and methyl orange (MO) in 100 μg/mL of silver colloidal (sample S, R and L) was added to the solutions respectively, organic dyes were constant for all the experiment. Effect of AgNPs dosages on degradation of MV, S, EMB and MO was studied with 20–100 ug/mL silver nanoparticles.

Results and Discussion

Characterization

(Figure 1) shows the UV–Vis spectra of silver colloids of S, R and L respectively. It is an important method to determine the
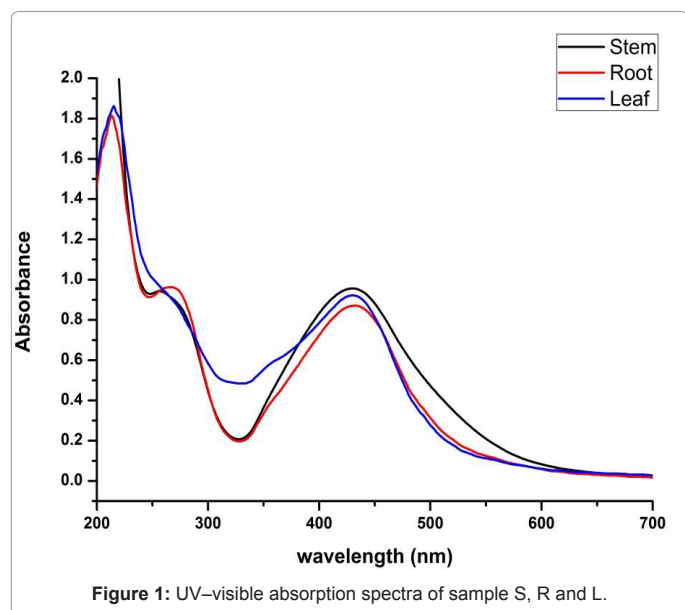
formation of metal nanoparticles in colloidal solution. It is observed that the maximum absorbance of Ag nanoparticles occurs at 430 nm. Appearance of this peak, assigned to a Surface Plasmon Resonance (SPR) band, is well-documented for various metal nanoparticles with different size range [20]. Formation of SPR is due to the particle shape, size, interaction with the medium and the degree of charge transfer between the particle and the medium.

FTIR spectrum was examined to identify the possible biomolecules responsible for capping and efficient stabilization of the biosynthesized Ag nanoparticles, which can help in further functionalization with other molecules for various applications in future. The IR spectrum of AgNPs shows intense bands at 3456.77 cm^{-1} (O-H, stretch, H-bonded) 29167.80 cm^{-1} (C-O stretch, free), 1634.37 cm^{-1} (C=C stretch) and 1045.22 cm^{-1}(C-F strong stretch). The IR spectrum of extract shows intense bands at IR spectrum of leaf extract shows 3456.77 cm^{-1}, 2916.80 cm^{-1}, 1634.37 cm^{-1} and 1045.22 cm^{-1} (Figure 2a), and significant variance was observed among the spectral positions of IR bands in extract and biosynthesized AgNPs owed to the reduction process. The presences of IR bands suggest the phenolics, alkaloids and terpenoids adsorbed on the surface of AgNPs [21]. The IR spectrum analysis also provided an idea about biomolecules bearing different functionalities which are present in the basic system. The possible mechanism for the reduction of Ag$^+$ to AgNPs is that phenolic OH groups present in hydrolysable tannins can form intermediate complexes with Ag$^+$ ions which consequently undergo oxidation to quinone forms with subsequent reduction of Ag$^+$ to Ag nanoparticles [22].

Analysis of AgNPs using X-ray diffraction confirmed the crystalline nature of particles (Figure 2b). A number of Bragg reflections with 2θ values of 32.414., 46.507, 57.937, 67.491 and 76.710 correspond to the (1 2 2), (2 3 1), (1 0 3), (1 0 6) and (3 1 1) set of lattice planes are observed which may be indexed as the band for face hexagonal shape in leaf mediated and stem bark and root mediated AgNPs centered cubic structure (ccs) (JCPDS file No. 41-1402) of silver. The unassigned peaks could be due to the crystallization of bioorganic phase that occurs on the surface of the nanoparticle.

The TEM images at different explant mediated synthesis of AgNPs and SAED pattern are presented in (Figure 3) (a-i), which give clear indications regarding structure, shape and particle size distribution. (Figure 3) (a–c) shows the TEM images of sample stem bark. TEM images of sample root and leaf shown in (Figure 3) (d-i). From the images, it can be seen that the particles are covered with extract it may be the phytoconstituents of extract (Figure 3 d&g). The SAED pattern of AgNPs reveals its polycrystalline nature. The average particle size calculated for sample S, R and L are 25.55 nm, 38.23 nm and 45.55 nm, respectively. The DLS pattern reveals that biosynthesized AgNPs of sample S, R and L shown in (Figure 4 a-c). DLS demonstrate the cubic shape and very narrow size distribution with polydispersity index (PDI) of all the samples. The sizes of the obtained particles of DLS are in good agreement with the values observed by TEM. Both DLS and TEM data confirm that the use of stem bark extract as reducing agents yields smaller particle sizes than using leaf and root extracts at the same concentration.

Catalytic degradation

Catalytic activities of biosynthesized AgNPs with different size and shapes of cubic sample S, R and L were evaluated using organic dyes such as methyl violet (MV), safranin (S), eosin methylene blue (EMB) and methyl orange (MO) aqueous solutions (50 mg/mL) as shown in (Figure 5).
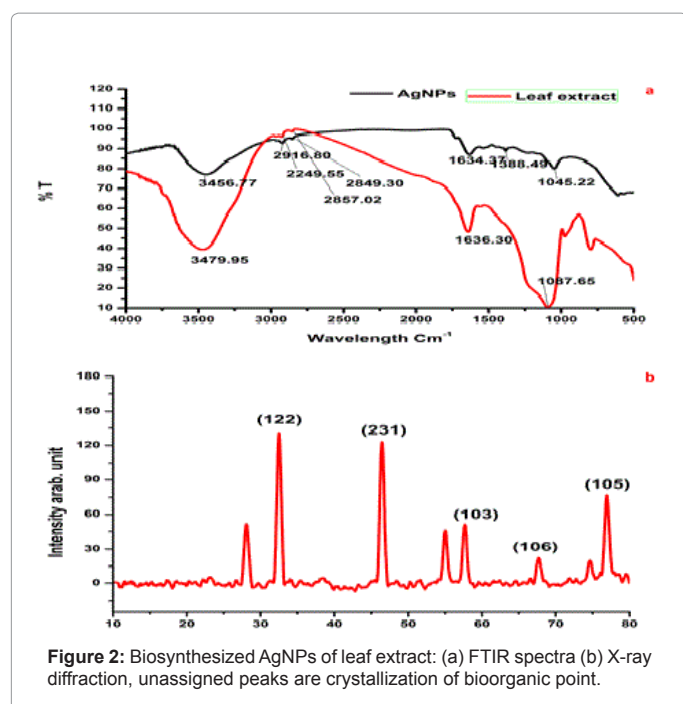

Figure 1: UV–visible absorption spectra of sample S, R and L.

Figure 2: Biosynthesized AgNPs of leaf extract: (a) FTIR spectra (b) X-ray diffraction, unassigned peaks are crystallization of bioorganic point.

Methylene violet (MV)

MV is a mixture of methylene blue and diluted alkalis that are mainly used as dyes for textiles to give deep violet. Based on the methyl groups Methylene violet function was varied. The relative absorbance of MV band was observed at 608 nm (Figure 6). After 30 min the addition of the sample S, R and L to the dye, the absorbance is gradually decreased and is shifted to higher wavelength. The decrease of absorbance is indicating the ability of phytoextract to degrade MV. System containing dye with different size of different explant extracts of AgNPs at the end of 30 min time interval showed a marked decrease in the absorbance of MV and increase of SPR peak of AgNPs. It reveals that the complete reduction of MV is accomplished in less than 30 min in the presence of AgNPs. The size and surface dependent photocatalytic property has been investigated for sample S, R and L. The photocatalytic degradation of MV in the presence of sample S, R and L AgNPs shown in Figure 6 a-c, respectively. Sample S and R is cubic nature and are small and have sharp edges and corners. In this region that atoms at these locations are likely to be both chemically very active and liable to dissolve easily, and that have the producing of very catalytically active sites. The fraction of atoms of cubic particles at these sites is probably generous, making these nanoparticles the most catalytically active [23]. The Hexagonal nanoparticles are the largest and most of its surface atoms are located on their (122) facets, which are known to be the least active. This explains their high value of activation energy. The "cubic" nanoparticles are have both the (111) and (200) facets with edges at the interfaces of these facets, explaining its catalytic activity [24].

Eosin methylene blue (EMB)

The EMB oxidation and reduction were carefully demonstrated recently from the electron (e⁻) reduction and oxidation abilities of EMB at ground state without using catalyzer $NaBH_4$ [25,26]. The photocatalytic activity of the AgNPs was investigated by choosing the photocatalytic degradation of EMB. The characteristic absorption peak at 430 nm of EMB was used for monitoring the catalytic degradation process. The absorption spectra of aqueous solution of EMB tested at different time intervals in the presence of S, R and L based AgNPs is shown in Figure 7. The main peak at 430 nm decreased gradually with the extension of the exposure time, indicating the photocatalytic degradation of EMB dye. As compared to the photocatalytic degradation with samples R and L, faster degradation kinetics and higher removal efficiencies were observed on sample S. Recent research reveals that photocatalytic activity of AgNPs can be strongly dependent on the structure, morphology, crystallographic nature and size of the particles [8,13].

Safarnin (S)

To test for the photodegradation of S dye by biosynthesized AgNPs of sample S, R and L, a solution containing S dye and sample S, R and L AgNPs is photoirradiated by sun light. At periodic intervals of time, aliquots of the sample were taken and the emission spectra were recorded. (Figure 8) show the quenching efficiency of S dye (50 mg/mL) in the presence of sample S, R and L degradation of dye. The reduction efficiencies of AgNPs increase with time, reaching a plateau. The degradation efficiency of S dye was possibly due to an increase of the applicable surface of the catalyst migration of holes to the surface of the AgNPs. It is important to note that degradation of the S dye in the absence of particles resulted in no significant change in the emission spectra. [27] states that Ag particles are highly efficient and stable catalysts with evident light source under controlled temperature; it induced visible light catalytic degradation and enhanced the visible light activity for degrading textile dyes and organic compounds.

Methylene orange (MO)

Photocatalytic degradation of MO dye was investigated by biosynthesized S, R and L AgNPs with solar irradiation technique by biometrically at different time intervals as shown in Figure 9. The characteristic absorption peak of MO solution was found to be 433 nm (Figure 5). Degradation of MO was visualized by decrease in peak intensity within 6 h of incubation time. There is no considerable shift in peak position for MO solution without exposure to biosynthesized AgNPs of sample S, R and L. Visible light was found to be faster in decolorizing dyes in the presence of metal catalyst [28,29]. The adsorption of AgNPs on to the MO solution was initially low and further increased with constant increase in time. The variation in the absorption intensity at 433 nm for samples S, R and L is rapid (Figure 9 a-c), signifying the faster reaction rate. The reaction rate (k) is comparatively larger for sample S having smaller particle size than that for sample L and R. The degradation was comparatively less for sample R as the particles are hexagonal. The degradation of the organic dyes increases with decrease in the size of the particles. The reducing in the structure of the metal particles favors the proliferation in the amount of the coordinate atoms and improves the adsorption of molecules on the surface of catalysts and thus improves the degradation of dyes [30]. Thus the catalytic activity of the silver nanoparticles was found to depend on the particle size and its shape.

The presence of silver nanoparticles with sun light was proven very effective for degradation of organic dyes. The linear correlation between ln (C/C_0) and the reaction time indicate the reduction process of organic dyes was a pseudo first order (inset of Figure 6-9 (a-c)). The result emphasize that the catalytic activity has been improved due to plant parts having different functional groups. In the present study AgNPs exhibit an awesome performance as a catalyst.

The effect of catalyst dosage varying from 20 to 100 μg/mL on
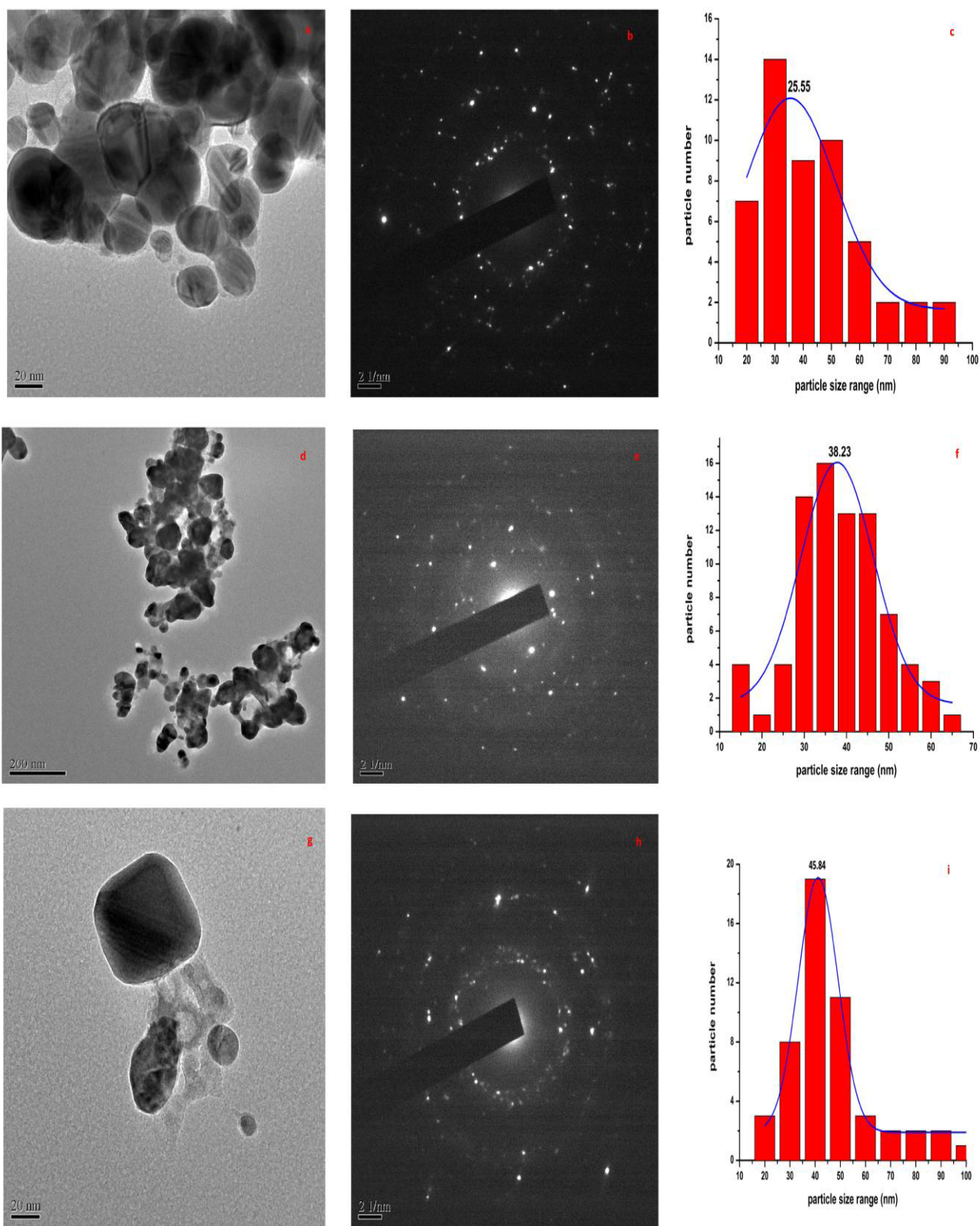
Figure 3: HRTEM images of sample S, R and L at different magnifications and SAED pattern. The image c, f and i shows the particle size distribution of sample S, R and L.
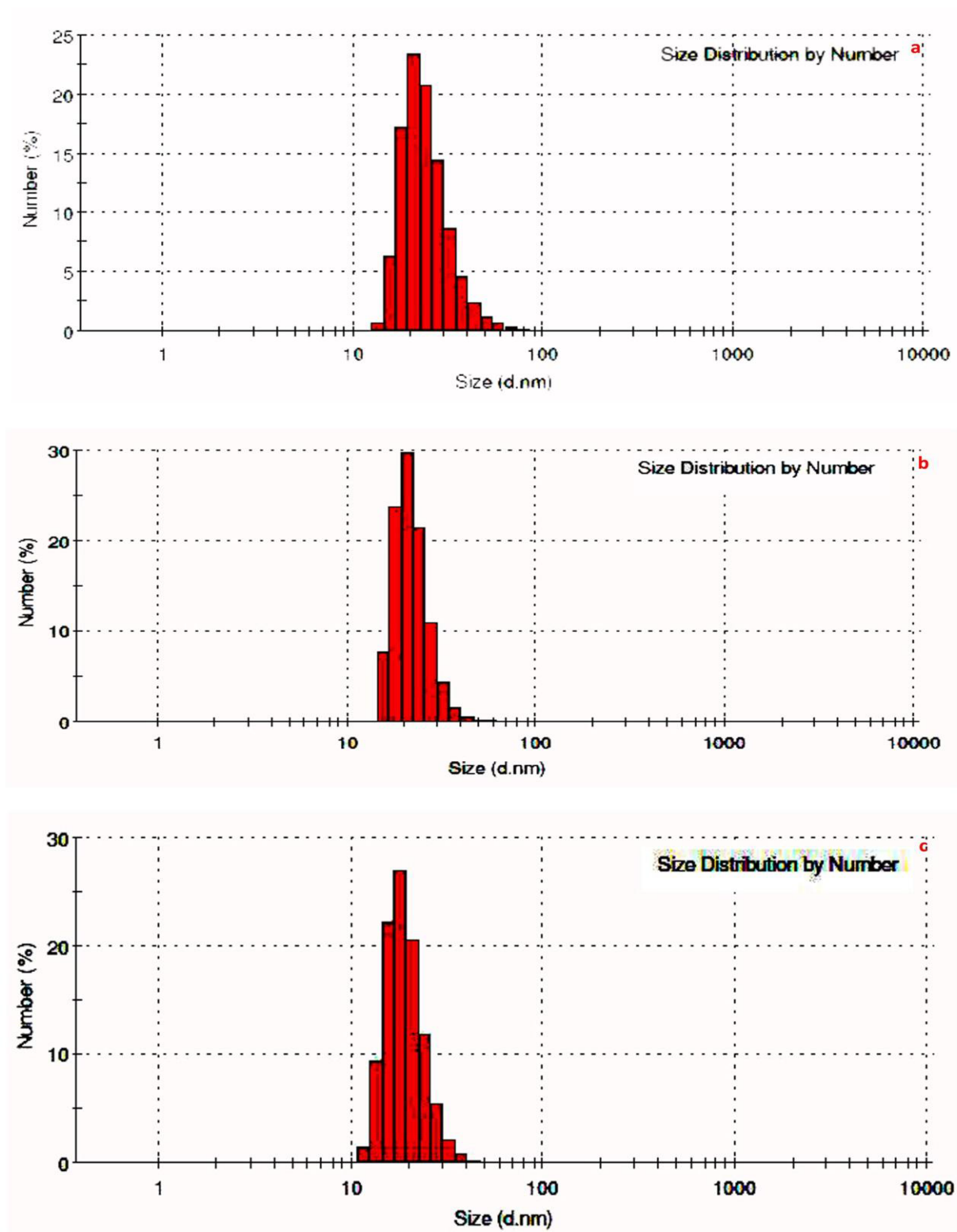
Figure 4: DLS of biosynthesized AgNPs: (a) stem bark (b) root (c) leaf.
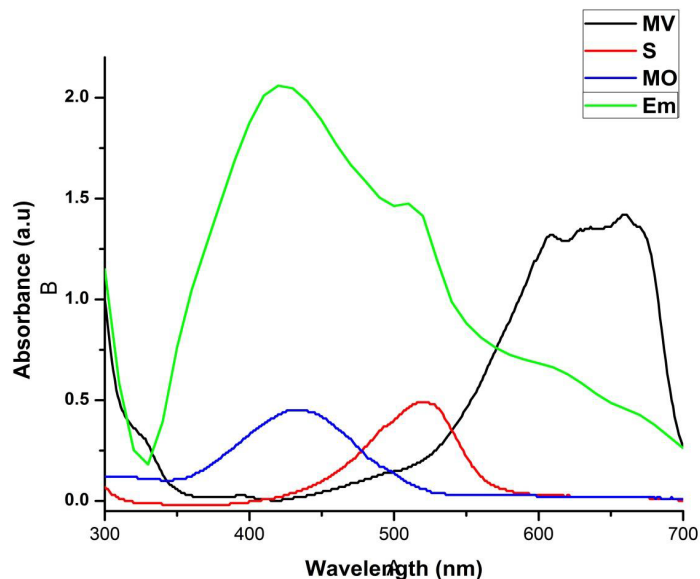
Figure 5: UV–visible absorption spectra of methylene violet (MV), safranin (S), eosin methylene blue (EMB) and methyl orange (MO) in the absence of biosynthesized AgNPs.
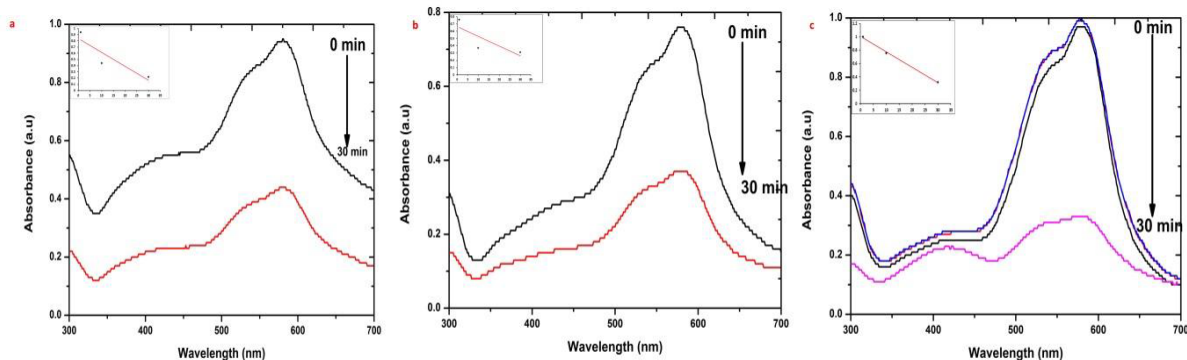

Figure 6: Effect of biosynthesized AgNPs on the catalysis of methylene violet (MV). UV–visible absorption spectra of degradation of MV inthe presence of (a) sample S (b) sample R and (c) sample L. (inset shows linear plots of ln (C/C0) with time of sample S, R and L, respectively).
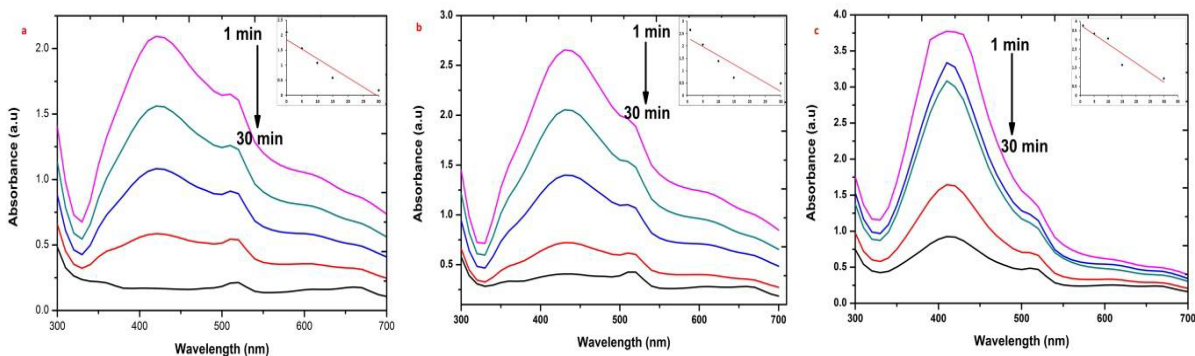

Figure 7: Effect of biosynthesized AgNPs on the degradation of eosin methylene blue (EMB) recorded for an interval of 30 min. UV–visible absorption spectra of degradation of EMB in the presence of (a) sample S (b) sample R and(c) sample L. (inset shows linear plots of ln (C/C0) with time of sample S, R and L, respectively).
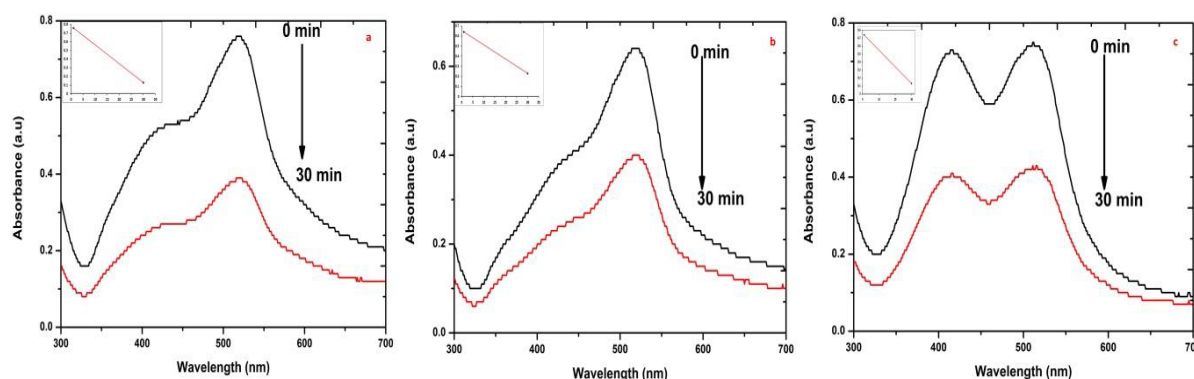
Figure 8: Effect of biosynthesized AgNPs on the degradation of safranin (S). UV–visible absorption spectra of degradation of dye S in the presence of (a) sample S (b) sample R and (c) sample L. (inset shows linear plots of ln (C/C0) with time of sample S, R and L, respectively).
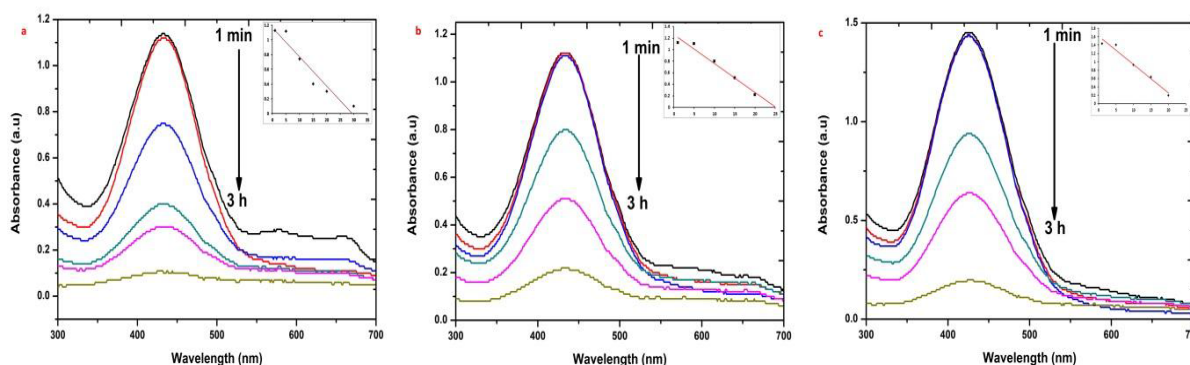

Figure 9: Effect of biosynthesized AgNPs on the reduction of methyl orange (MO). UV–visible absorption spectra of degradation of MO in the presence of (a) sample S (b) sample R and (c) sample L. (inset shows linear plots of ln (C/C0) with time of sample S, R and L, respectively).

degradation of different organic dyes with different biosynthesized AgNPs was analyzed keeping the other parameters constant. The degradation of organic dyes showed enhancement in the rate of degradation with respect to the increasing AgNPs concentration of sample S, R and L (Figure 10 (a-l)). Increasing the catalyst dose of 20 to 100 µg/mL the degradation rate was increased up to 100% was observed in sample S in EMB and approximately 95% degradation for 100 µg/mL dose of sample R and L. The varied concentration of silver nanoparticles showed higher degradation with increase in catalyst concentration was due to the increase in the number of reaction sites. In this study we observed that increasing the biosynthesized AgNPs dosages the degradation rate was also increased in all the organic dyes with respective samples.

During degradation the catalysis was occurs on the surface region of metals, therefore increasing the surface area availability will significantly improve the efficiency of the catalyst. Decreasing the particle size will increase the catalytic activity, but there is a critical size below which proves that further decreases will actually hamper the reaction [31]. Metal nanoparticles support the electron (e^-) relay from the donor to the acceptor and act as a substrate for the e^- transfer reaction. During e^- transfer reaction, the reactants are adsorbed on the surface of metal and consequently, the reactants gain an e^- and is reduced. Thus AgNPs act as an efficient catalyst through the electron transfer process in all the above catalytic reactions [32].

Conclusion

For a healthy future of nanotechnology, green synthetic strategy should be adopted for nanoparticles synthesis by using eco-friendly and renewable molecules to get rid of hazards arising out of the use of chemical reducing agents and organic solvents. Colloid based nanotechnology has been developed to control the size, shape, uniformity and functionality. The biosynthesized AgNPs exhibits a very high degradation activity under visible light source. In the present manuscript, we have demonstrated the synthesis of silver nanoparticles with different extract of *H. isora*. The present synthesis method proved to be helpful to reduced synthesis of AgNPs and their reduction properties. The bioreduced AgNPs exhibited remarkable degradation properties in a reduction of organic dyes, methyl violet (MV), safranin (S), eosin methylene blue (EMB) and methyl orange (MO). The explant dependent (size was dependent on explant type) catalytic activity was also observed in the biosynthesized AgNPs. This new green chemistry holds several valuable attractions and offers an effective and economic way to environmental bioremediation protection.
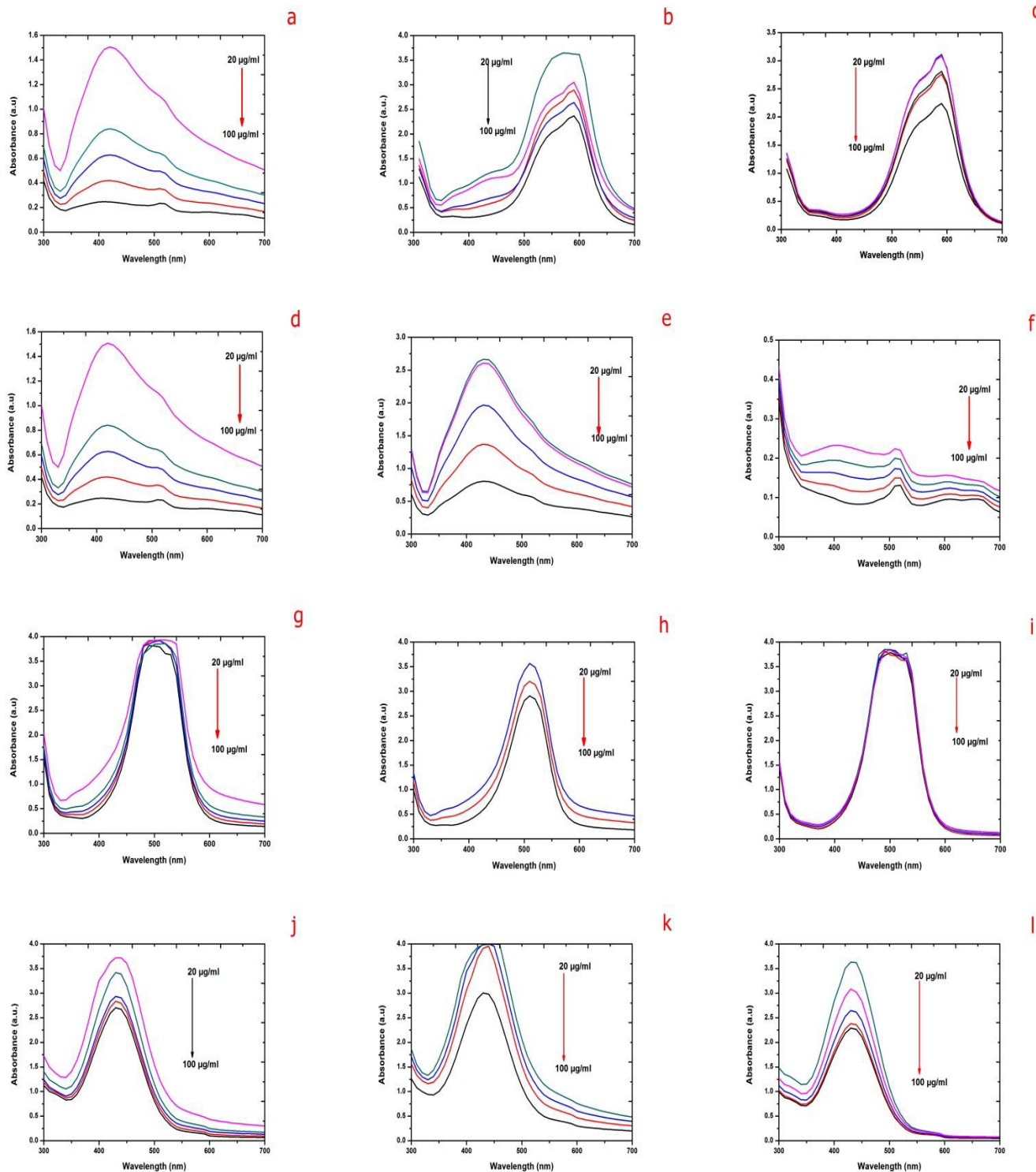
Acknowledgements

Figure 10: Effect of biosynthesized dosages on degradation of dyes: degradation of MV (a- Sample S; b- Sample R; c- sample L); degradation EMB (d- Sample S; e- Sample R; f- sample L); degrdation of S (g- Sample S; h- Sample R; i- sample L); degrdation of MO (j- Sample S; k- Sample R; l- sample L).

References

1. Faisal M, Tariq MA, Muneer M (2007) Photocatalysed degradation of two selected dyes in UV-irradiated aqueous suspensions of titania. Dyes Pigm 72: 233–239.

2. Tang WZ, An H (1995) UV/TiO2 photocatalytic oxidationofcommercialdyesin aqueous solutions. Chemosphere 31: 4157–4170.

3. Sobana N, Muruganadham M, Swaminathan M (2006) Nano-Ag particles doped TiO2 for efficient photodegradation of Direct azo dyes. J Mol Catal A 258: 124–132.

4. El-Kemary M, Abdel-Moneam Y, Madkour M, El-Mehasseb I (2011) Enhanced photocatalytic degradation of Safranin-O by heterogeneous nanoparticles for environmental applications. J Lumin 131: 570-576.

5. Ullah R, Dutta J (2008) Photocatalytic degradation of organic dyes with manganese-doped ZnO nanoparticles. J Hazard Mater 156: 194-200.

6. Wu ZC, Zhang Y, Tao TX, Zhang L, Fong H (2010) Silver nanoparticles on amidoxime fibers for photo-catalytic degradation of organic dyes in waste water. Appl Surf Sci 257: 1092-1097.

7. Arunachalam R, Dhanasingh S, Kalimuthu B, Uthirappan M, Rose C, et al. (2012) Phytosynthesis of silver nanoparticles using *Coccinia grandis* leaf extract and its application in the photocatalytic degradation. Colloids Surf B Biointerfaces 94: 226-230.

8. Suvith VS, Philip D (2014) Catalytic degradation of methylene blue using biosynthesized gold and silver nanoparticles. Spectrochim Acta A Mol Biomol Spectrosc 118: 526-532.

9. Njagi EC, Huang H, Stafford L, Genuino H, Galindo HM, et al. (2010) Biosynthesis of iron and silver nanoparticles at room temperature using aqueous sorghum bran extracts. Langmuir 27: 264-271.

10. Nosaka Y, Matsushita M, Nishino J, Nosaka AY (2005) Nitrogen-doped titanium dioxide photocatalysts for visible response prepared by using organic compounds. Sci Technol Adv Mater 6: 143-148.

11. Huang YU, Zheng X, Zhongyi YIN, Feng TAG, Beibei FANG, et al. (2007) Preparation of nitrogen-doped TiO_2 nanoparticle catalyst and its catalytic activity under visible light. Chin J Chem Eng 15: 802-807.

12. Ghosh SK, Kundu S, Mandal M, Pal T (2002) Silver and gold nanocluster catalyzed reduction of methylene blue by arsine in a micellar medium, Langmuir 18: 8756–8760.

13. Vidhu VK, Philip D (2014) Catalytic degradation of organic dyes using biosynthesized silver nanoparticles. Micron 56: 54-62.

14. Mathew PJ, Unnithan MC (1992) Search for plant having anticancer properties used by the tribal of Wynadu, Malappuram and Palghat districts of Kerala, India. Aryavaidyan 6: 54-60.

15. Shriram V, Kumar V, Shitole MG, Shriram V, Kumar V, et al. (2008) Indirect organogenesis and plant regeneration in *Helicteres isora* L. an important medicinal plant. In Vitro Cell Dev Biol Plant 44: 186–193.

16. Singh SB, Singh AK, Thakur RS (1984) Chemical constituents of the leaves of Helicteres isora. Ind J Pharmaceu Sci 46: 148-149.

17. Kumar G, Banu GS, Murugesan AG, Rajasekara-Pandian M (2007) Preliminary toxicity and phytochemical studies of aqueous bark extract of *Helicteres isora* L. Int J Pharm 3: 96–100.

18. Venkadesh S, Reddy GD, Reddy YSR, Sathyavathy D, Reddy BM (2004) Effect of *Helicteres isora* root extracts on glucose tolerance in glucose-induced hyperglycemic rats. Fitoterapia 75: 364–367.

19. Bhakya S, Muthukrishnan S, Sukumaran M, Muthukumar M (2015) Biogenic synthesis of silver nanoparticles and their antioxidant and antibacterial activity. App Nanosci 1-12.

20. Muthukrishnan S, Bhakya S, Kumar TS, Rao MV (2015) Biosynthesis, characterization and antibacterial effect of plant-mediated silver nanoparticles using *Ceropegia thwaitesii*–An endemic species. Ind Crops Prod 63: 119-124.

21. Nithya Deva Krupa A, Raghavan V (2014) Biosynthesis of Silver Nanoparticles Using *Aegle marmelos* (Bael) Fruit Extract and Its Application to Prevent Adhesion of Bacteria: A Strategy to Control Microfouling. Bioinorg Chem Appl 2014.

22. Fayaz AM, Balaji K, Girilal M, Yadav R, Kalaichelvan PT, et al. (2010) Biogenic synthesis of silver nanoparticles and their synergistic effect with antibiotics: a study against gram-positive and gram-negative bacteria. Nanomedicine 6: 103-109.

23. Somorjai GA (1994) Introduction to Surface Chemistry and Catalysis; Wiley Publishers: New York.

24. Xu Z, Xiao FS, Purnell SK, Alexeev O, Kawi S (1994) Size-dependent catalytic activity of supported metal clusters. Nature 372: 346-348.

25. Abe M, Kubo A, Yamamoto S, Hatoh Y, Murai M, et al. (2008) Dynamic function of the spacer region of acetogenins in the inhibition of bovine mitochondrial NADH-ubiquinone oxidoreductase (complex I). Biochemistry 47: 6260–6266.

26. Santhanalakshmi J, Venkatesan P (2011) Mono and bimetallic nanoparticles of gold, silver and palladium-catalyzed NADH oxidation-coupled reduction of Eosin-Y. J Nanoparticle Res 13: 479-490.

27. Ansari SA, Khan MM, Ansari MO, Lee J, Cho MH (2013) Biogenic synthesis, photocatalytic, and photoelectrochemical performance of Ag–ZnO nanocomposite. J Phys Chem C 117: 27023-27030.

28. Zhao J, Chen C, Ma W (2005) Photocatalytic degradation of organic pollutants under visible light irradiation. Topics in Catal 35: 269-278.

29. Ge L, Han C, Liu J (2011) Novel visible light-induced gC 3 N 4/Bi 2 WO 6 composite photocatalysts for efficient degradation of methyl orange. Appl Catal B 108: 100-107.

30. Falicov LM, Somorjai GA (1985) Correlation between catalytic activity and bonding and coordination number of atoms and molecules on transition metal surfaces: Theory and experimental evidence. Proc Natl Acad Sci India Sect B Biol Sci 82: 2207-2211.

31. Grogger C, Fattakhov SG, Jouikov VV, Shulaeva MM, Reznik VS (2004) Primary steps of oxidation and electronic interactions in anodic cleavage of α,ω-diisocyanurate substituted dialkyl disulfides. Electrochimica Acta 49: 3185-3194.

32. Christopher P, Xin H, Linic S (2011) Visible-light-enhanced catalytic oxidation reactions on plasmonic silver nanostructures. Nat Chem 3: 467-472.